nature chemical biology

ARTICLE

PUBLISHED ONLINE: 10 JANUARY 2010 | DOI: 10.1038/NCHEMBIO.293

The p110δ structure: mechanisms for selectivity and potency of new PI(3)K inhibitors

Alex Berndt[1], Simon Miller[1], Olusegun Williams[2], Daniel D Le[2], Benjamin T Houseman[2], Joseph I Pacold[1], Fabrice Gorrec[1], Wai-Ching Hon[1], Pingda Ren[3], Yi Liu[3], Christian Rommel[3], Pascale Gaillard[4], Thomas Rückle[4], Matthias K Schwarz[4], Kevan M Shokat[2], Jeffrey P Shaw[4] & Roger L Williams[1]*

Deregulation of the phosphoinositide-3-OH kinase (PI(3)K) pathway has been implicated in numerous pathologies including cancer, diabetes, thrombosis, rheumatoid arthritis and asthma. Recently, small-molecule and ATP-competitive PI(3)K inhibitors with a wide range of selectivities have entered clinical development. In order to understand the mechanisms underlying the isoform selectivity of these inhibitors, we developed a new expression strategy that enabled us to determine to our knowledge the first crystal structure of the catalytic subunit of the class IA PI(3)K p110δ. Structures of this enzyme in complex with a broad panel of isoform- and pan-selective class I PI(3)K inhibitors reveal that selectivity toward p110δ can be achieved by exploiting its conformational flexibility and the sequence diversity of active site residues that do not contact ATP. We have used these observations to rationalize and synthesize highly selective inhibitors for p110δ with greatly improved potencies.

The PI(3)Ks are structurally closely related lipid kinases that catalyze the ATP-dependent phosphorylation of phosphoinositide substrates[1,2]. Together with the serine/threonine protein kinase B (PKB), PI(3)Ks constitute a central signaling hub that mediates many diverse and crucial cell functions, including cell growth, proliferation, metabolism and survival[1,3]. The observation that PI(3)Ks acting downstream of receptor tyrosine kinases (RTKs) are the most commonly mutated kinases in human cancers has spurred interest in understanding the structural mechanisms for how these mutations upregulate PI(3)K activity and in developing selective and drug-like PI(3)K inhibitors[4,5].

PI(3)Ks can be grouped into three classes based on their domain organization[6]. Class I PI(3)Ks are heterodimers consisting of a p110 catalytic subunit and a regulatory subunit of either the 'p85' type (associated with the class IA p110 isoforms p110α, p110β or p110δ) or the 'p101' type (associated with the class IB p110 isoform p110γ). The p110 catalytic subunit consists of an adaptor-binding domain (ABD), a Ras-binding domain (RBD), a C2 domain, a helical domain and the kinase domain[7–10].

Mutant mice and inhibitor studies have shown less functional redundancy for the various class I PI(3)K isoforms than previously anticipated. Whereas p110α and p110β are ubiquitously expressed, p110γ and p110δ are predominantly found in hematopoietic cells[11–13]. Genetic deregulation of PI(3)K activity (oncogenic gain-of-function mutations, overexpression) has been implicated in cancer (all class I PI(3)K isoforms)[14–17], diabetes (p110α)[18], thrombosis (p110β)[19], rheumatoid arthritis (p110γ and p110δ)[20] and asthma (p110γ and p110δ)[21,22]. Consequently, the selective inhibition of individual PI(3)K isoforms using small-molecule and ATP-competitive inhibitors is a promising therapeutic strategy[23]. However, because all active site side chains in contact with ATP are completely conserved throughout all class I PI(3)K family members (**Supplementary Fig. 1**), this remains a challenging objective. Furthermore, in order to minimize undesired and often poorly understood toxic side effects, such inhibitors ideally would have to show no cross-reactivity toward off-pathway targets[24].

The earliest generation of small-molecule and ATP-competitive PI(3)K inhibitors, including the pan-selective LY294004 (ref. 25) and wortmannin[26], were important tools for investigating PI(3)K-mediated cellular responses in the laboratory, but their low affinity (LY294002), instability (wortmannin), nonselectivity and toxicity limited their clinical use. However, further chemical modifications of some of these early inhibitors significantly helped to improve their drug-like properties. For example, PWT-458 (Wyeth) and PX-866 (Oncothyreon) are modified wortmannin-based PI(3)K inhibitors with improved pharmacological properties that are currently in phase 1 clinical trials[27,28].

The first crystal structures of p110γ in complexes with pan-selective PI(3)K inhibitors[29] made it possible to begin to rationalize PI(3)K isoform-selective inhibitors such as AS604850 (Merck-Serono) for p110γ (ref. 30). However, many of these inhibitors retained off-target activities, and, partially due to the lack of crystal structures of other PI(3)K isoforms and PI(3)K-related protein kinases (PIKKS), these unwanted side effects were difficult to rationalize.

Notably, the development of multi- and pan-selective PI(3)K inhibitors as well as dual PI(3)K/mTOR or PI(3)K/tyrosine kinase inhibitors[31] rather than isoform-selective PI(3)K inhibitors remains a valid therapeutic strategy. XL-147 (Exelixes), which is currently evaluated in combination with other cancer therapeutics, is in phase 1 and 2 clinical trials for the treatment of non-small-cell lung cancer. GDC-0941 (Roche)[32] is also in phase 1 trials for the treatment of breast cancer[33]; both XL-147 and GDC-0941 are examples of pan class I–selective PI(3)K inhibitors. NVP-BEZ235 (Novartis), which is currently in phase 1 and 2 trials for breast cancer[34], and SF1126 (Semaphore), an RGDS peptide–conjugated prodrug of LY294002 presently in phase 1 trials[35], are examples of dual-selectivity PI(3)K/mTOR inhibitors.

Recently, several new class I PI(3)K isoform-selective inhibitors showing improved selectivities and potencies have been reported, and some of them have entered clinical trials: CAL-101 (Calistoga), a derivative of the highly p110δ-selective inhibitor IC87114 (ref. 36) with increased potency, entered phase 1 for the treatment of acute

[1]Medical Research Council-Laboratory of Molecular Biology, Cambridge, UK. [2]Howard Hughes Medical Institute and Department of Cellular and Molecular Pharmacology, University of California, San Francisco, California, USA. [3]Intellikine Inc., La Jolla, California, USA. [4]Merck-Serono Research Center, Geneva, Switzerland. *e-mail: rlw@mrc-lmb.cam.ac.uk

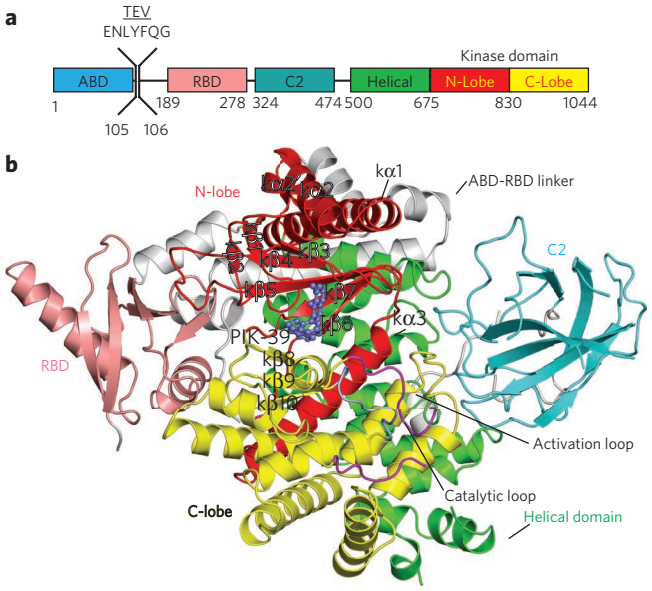

Figure 1 | Domain organization, construct design and overall crystal structure of p110δ. (**a**) A TEV protease cleavage site was introduced between residues 105 and 106 of the p110δ ABD-RBD linker. The numbers below the boxes correspond to the indicated domain boundaries. After purification of the p110δ-iSH2 complex, the catalytic core is released by cleavage with TEV protease. (**b**) Cartoon representation of the overall cocrystal structure of the ΔABDp110δ–PIK-39 complex. Linker regions are colored in white, the RBD in salmon, the C2 domain in cyan, the helical domain in green, the kinase domain N-lobe in red and the kinase domain C-lobe in yellow. PIK-39 is shown in light blue as a ball-and-stick representation. Selected secondary structure elements of the kinase domain are labeled.

myeloid leukemia (AML) and B-cell chronic lymphoid leukemia (CLL). The p110β-selective AZD6482 (AstraZeneca) is in phase 1 trials for the treatment of thrombosis. Notably, however, despite a growing list of such isoform-selective compounds, little is known about what determines isoform selectivity on a structural level.

Impaired PI(3)Kδ signaling results in severe defects of innate and adaptive immune responses, suggesting that targeting of this isoform would be a beneficial therapeutic strategy[20,24]. To elucidate the molecular mechanisms of isoform selectivity of PI(3)Kδ inhibitors, we report the crystal structure of the p110δ catalytic core, both free and in complexes with a broad panel of new and mostly p110δ-selective PI(3)K inhibitors. Our study provides the first detailed structural insights into the active site of a class IA PI(3)K occupied by noncovalently bound inhibitors. Furthermore, our structures suggest mechanisms to achieve p110δ selectivity and to increase the potency of inhibitors without sacrificing isoform selectivity. To obtain these structures, we developed a unique expression and purification scheme that has now been extended to all class IA PI(3)K isoforms.

With our new set of p110δ crystal structures and better models of flexibility resulting from molecular dynamics simulations, we are now starting to understand why p110δ can be more easily deformed to open an allosteric pocket in which p110δ-selective inhibitors can be accommodated.

RESULTS

Expression and catalytic activity of ΔABDp110δ

Our initial attempts to express either the full-length or the ABD-truncated p110δ catalytic subunit in Sf9 cells produced only insoluble protein. However, we could readily express and purify p110δ in complexes with only the iSH2 domain of p85α. We devised a new expression and purification strategy by introducing a TEV protease cleavage site in the linker region between the ABD and the RBD of p110δ (**Fig. 1a**) with the objective of generating an ABD-truncated version of this isoform for crystallization trials. The ΔABDp110δ construct showed a considerably enhanced lipid kinase activity *in vitro* when compared with either the holo p110δ-p85α complex or the p110δ-p85α nicSH2 complex (**Supplementary Fig. 2**).

Overall structure of ΔABDp110δ

Crystallographic statistics for all p110δ datasets are given in **Supplementary Table 1**. The overall fold of p110δ is very similar to the catalytic subunits of p110γ and p110α (**Fig. 1b**)[8,37]. Helices Lα1–Lα3 of the ABD-RBD linker pack tightly against the helical domain, and stretch from the RBD to the C2 domain. The helices kα1 and kα2/kα2' of the kinase domain form a hairpin in the N-lobe that sits on top of a five-stranded β-sheet formed by kβ3–kβ7, and this hairpin structurally distinguishes PI(3)Ks from protein kinases. These latter helices seem to extend the antiparallel A/B pairs of α-helices found in the helical domain. The kinase domain has an extensive, tightly packed interface with the helical domain. All of the catalytically important motifs within this domain are well ordered, with the exception of residues 920–928 of a region known as the "activation" or phosphoinositide-binding loop. Notably, the residues within the p110δ 893-DRH-895 motif located in the "catalytic" loop, a motif conserved in all PI(3)Ks and inverted (HRD) in protein kinases, adopt a different conformation from what was previously observed in the structure of p110γ (**Supplementary Fig. 3**)[8]. This different conformation might be critical for the correct positioning of the DFG aspartate at the beginning of the activation loop.

All the domains of p110δ superimpose closely on previously reported PI(3)K structures (**Supplementary Fig. 4a–f**). However, the most noteworthy difference in the overall structure of p110δ relative to p110α or p110γ is a change in the orientation of the N-lobe with respect to the C-lobe of the kinase domain. This shift may reflect motions characteristic of the catalytic cycle, analogous to the hinging and sliding motions of the N- and C-lobes that have been described for protein kinases[38]. Furthermore, the RBD shifts relative to the N-lobe of the kinase domain (**Supplementary Fig. 4g**). The RBD mediates interaction with Ras in a GTP-dependent manner for all three isoforms[11,12,39,40]. Despite the great sequence divergence among the isoforms in the RBD, the overall RBD backbone conformation is very closely preserved among the various class I isoforms (**Supplementary Fig. 4f**). However, differences in the orientation of the RBD relative to the kinase domain suggest the possibility of different mechanisms of activation by Ras. The conformation of the loop connecting kβ4 and kβ5 (Tyr763 to Val774 in p110δ) in the N-lobe is different in all the isoforms (longest in p110α, shortest in p110δ), and this correlates with the orientation of the RBD. Within the RBD of p110δ, residues 231–234 are disordered. The equivalent region in p110α is an ordered helix (Rα2), whereas in p110γ this region is ordered only in the Ras-p110γ complex, although it has a completely different conformation than in p110α.

Cocrystallization of p110δ with inhibitors

We chose a set of chemically diverse inhibitors in order to understand the structural mechanisms that underlie p110δ-specific inhibition in contrast to broadly specific PI(3)K inhibitors. Even though we obtained crystals grown in the presence of ATP, only a weak density somewhat larger than what would be expected for an ordered water molecule was observed in the hinge region. We will refer to this structure as the apo form of p110δ.

ATP-binding pocket

All of the compounds presented here contact a core set of six residues in the ATP-binding pocket (**Supplementary Table 2**), and—apart from the hinge residue Val827 in p110δ—these residues are invariant in all of the class I PI(3)K isotypes. Based on our

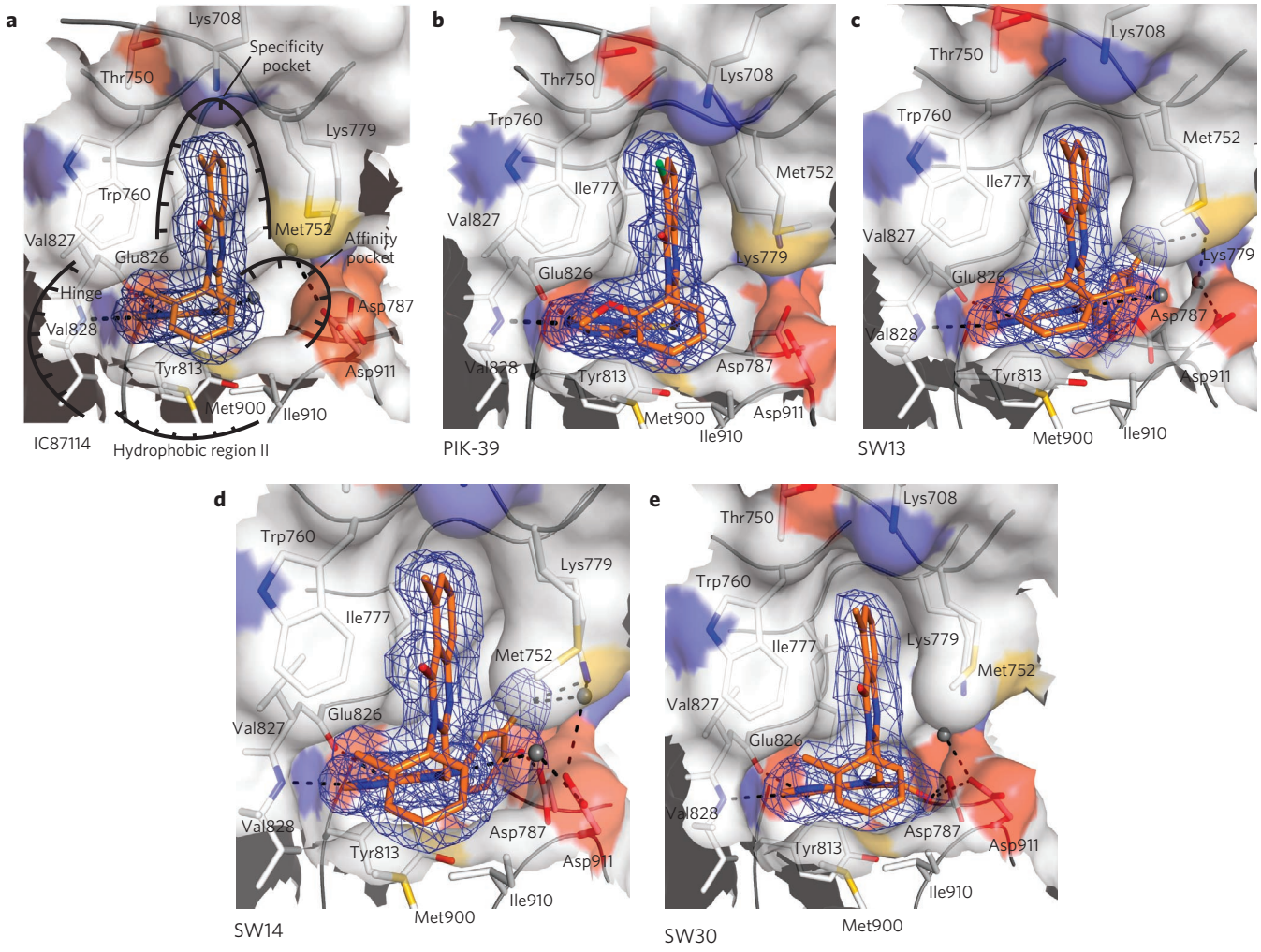

Figure 2 | The propeller-shaped p110δ-selective inhibitors induce the formation of the specificity pocket. (**a**–**e**) Shown are the active sites of p110δ in complex with the inhibitors IC87114 (**a**), PIK-39 (**b**), SW13 (**c**), SW14 (**d**) and SW30 (**e**). Key residues that outline the active site and interact with the compounds and the $2mF_o - DF_c$ electron densities (contouring level 1σ) are presented. Selected water molecules in the active sites are shown as gray spheres. Note that IC87114 and PIK-39 do not fill the affinity pocket, whereas SW13, SW14 and SW30 do. Dashed black lines represent hydrogen bonds.

inhibitor-bound structures of p110δ as well as previously described PI(3)K complexes[18,29,30,32,41], we can define four regions within the ATP-binding pocket that are important for inhibitor binding (**Fig. 2a**): an "adenine" pocket (hinge), a "specificity" pocket, an "affinity" pocket and the hydrophobic region II located at the mouth of the active site[18,42]. Of the core active site residues, only two are in contact with inhibitors in all complexes: Val828 and Ile910. Residues 825–828 line the adenine pocket and form a hinge between the N-lobe and C-lobe of the catalytic domain. The backbone amide of the hinge Val828 makes a characteristic hydrogen bond in all of the p110-inhibitor complexes. Additionally, the backbone carbonyl of hinge Glu826 establishes hydrogen bonds to most of the inhibitors.

Our selection of inhibitors can be organized into three types. The first type includes inhibitors that adopt a propeller-shaped conformation (two roughly orthogonally oriented aromatic ring systems) when bound to the enzyme (**Fig. 2a–e** and **Supplementary Fig. 5**). These are mostly p110δ-selective inhibitors that stabilize a conformational change that opens a hydrophobic "specificity" pocket in the active site that is not present in the apo structure of the enzyme as previously reported for the p110γ–PIK-39 crystal structure[18]. We also cocrystallized the p110δ enzyme with a second set of mostly flat and multi- to pan-selective class I PI(3)K inhibitors that do not provoke such a conformational rearrangement. AS15, which has a distorted propeller shape when bound to the enzyme, is the only example of a third type of inhibitor that is highly selective for the p110δ isoform, although it does not open the specificity pocket.

The propeller-shaped inhibitors IC87114 and PIK-39

The discovery of the p110δ-selective inhibitor IC87114 (ICOS) in 2003 (ref. 36) was a proof of principle that isoform selectivity of PI(3)K inhibitors can be accomplished, and so far it remains one of the most selective p110δ inhibitors known.

The crystal structures of the p110δ-IC87114 (**1**) (**Fig. 2a**) and the p110δ–PIK-39 (**2**) (**Fig. 2b**) complexes show that the purine group of the compounds resides within the adenine pocket and establishes hydrogen bonds to the hinge residues Glu826 and Val828. The quinazolinone moiety is sandwiched into the induced hydrophobic specificity pocket between Trp760 and Ile777 on one side and two P-loop residues, Met752 and Pro758, on the other side. The specificity pocket is not present in the apo enzyme where the P-loop Met752 rests in its "in" position leaning against Trp760. The toluene group (IC87114) and the methoxyphenyl group (PIK-39) attached to the quinazolinone moiety project out of the ATP-binding pocket over a region that we will refer to as hydrophobic region II.

PIK-39 binding to both p110δ and p110γ induces a slight opening in the ATP-binding pocket. The p110δ ATP-binding pocket accommodates the PIK-39–induced conformational change by a

local change in the conformation of the P-loop (residues 752–758 in p110δ), whereas the equivalent opening of the p110γ pocket is accompanied by a conformational change that involves much of the N-lobe moving with respect to the C-lobe. The loop between kα1 and kα2 of p110γ (residues 752–760) sits on top of the P-loop (residues 803–811) and appears to rigidify it, so that the compound-induced opening of the pocket is accompanied by a shift of the N-lobe as a unit (**Supplementary Fig. 6** and **Supplementary Movies 1** and **2**). In contrast to p110γ, in p110δ the slightly shorter kα1-kα2 loop leaves the P-loop largely free and able to move independently of the rest of the N-lobe. We proposed that opening of the specificity pocket might be easier in p110δ compared to p110γ.

Molecular dynamics simulations of p110δ and p110γ

Perturbation analysis by molecular dynamics simulations suggests that the free energy of the specificity pocket closure is more favorable in p110γ than p110δ (**Supplementary Fig. 7**). To quantify the higher degree of flexibility within the p110δ active site, we performed molecular dynamics simulations of the apo enzymes of both isoforms (see **Supplementary Methods** and **Supplementary Movies 3** and **4**). The potential energy of the interaction of PIK-39 with the enzyme is more favorable for p110δ than for p110γ (**Supplementary Fig. 8**). Our results further show that the distance between Trp760 (Trp812 in p110γ) and the P-loop Met752 (Met804 in p110γ) does not change appreciably in p110δ over the course of the simulation because the conformational changes observed for both residues are synchronized with each other—that is, the tryptophan smoothly follows the methionine and vice versa. In contrast, in p110γ, as the Met804 transiently assumes alternate rotamers, it briefly creates gaps between itself and Trp812. Trp812 of p110γ is sterically constrained by a hydrogen bond to Glu814 (Met762 in p110δ) and is therefore unable to flex in synchrony with Met804 as in p110δ. Additionally, in p110γ there is a more pronounced hydrophobic interaction between the Trp812 and the hinge Ile881, which might further restrain the position of the tryptophan. The transient opening of the specificity pocket in p110γ would allow water to become trapped, leading to an unfavorable entropy change.

Increased potencies of propeller-shaped inhibitors

The SW series (**3**, **4** and **5**)[43] and INK series (**6** and **7**) of inhibitors take advantage of both the specificity pocket and the affinity pocket (synthesis details for these compounds are given in the **Supplementary Methods**). This pocket is lined by a thin hydrophobic strip formed by Leu784, Cys815 and Ile825 at the back of

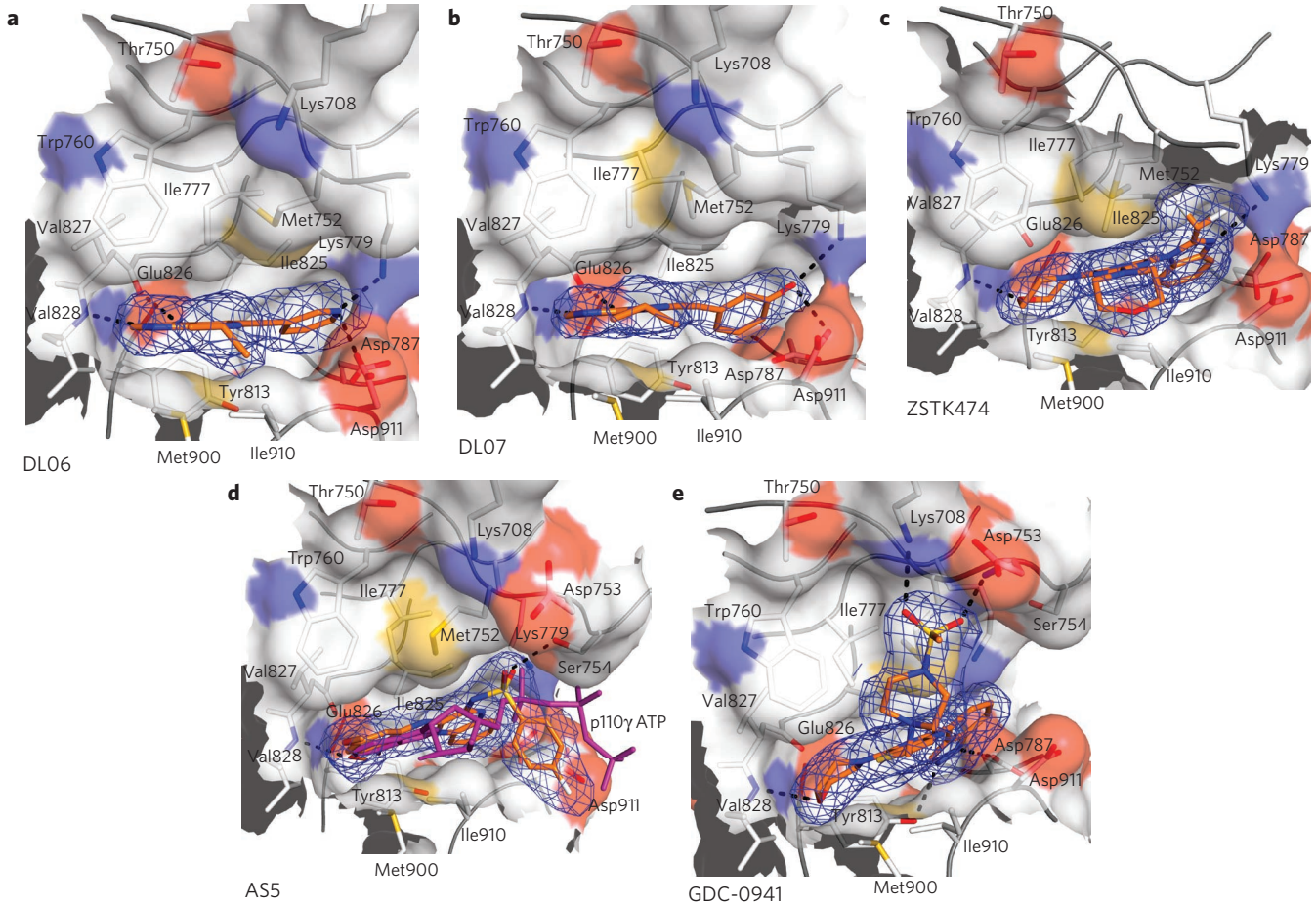

Figure 3 | The flat inhibitors DL06, DL07, ZSTK474, AS5 and GDC-0941 are multi- to pan-selective class I PI(3)K inhibitors that do not induce the opening of the specificity pocket. (**a**–**e**) Shown are the binding modes of DL06 (**a**), DL07 (**b**), ZSTK474 (**c**), AS5 (**d**) and GDC-0941 (**e**) in the active site of p110δ. Met752 is in its 'in' position for all these compounds. For **d**, the structure of the p110γ-ATP complex (Protein Data Bank entry 1E8X) was superimposed on the C_α-backbone of p110δ to show the proximity of the sulfonyl group of AS5 to the α-phosphate group of ATP (purple). This sulfonyl group is a hydrogen bond acceptor to Ser754 located in the P-loop of p110δ. (**e**) GDC-0941 is a pan-class IA PI(3)K inhibitor that (like AS15) interacts with residues outside the active site. GDC-0941 occupies the adenine pocket and the affinity pocket within the active site of p110δ and engages there in hydrogen bonds with Val828, Tyr813 and Asp787. Additionally, the substituted piperazine group of GDC-0941 extends out of the ATP-binding site where its methylsulfonyl moiety acts as a hydrogen bond acceptor for Asp753 of the P-loop and Lys708 at the beginning of kα2. The contouring level of the $2mF_o - DF_c$ electron densities is 1σ for each compound.

the ATP-binding pocket and flanked on the top by the side chains of Pro758 and Lys779 and on the bottom by Asp787 (hydrophobic region I in protein kinases). These mostly p110δ-selective compounds (SW14 is dual-selective for p110γ and p110δ) are also propeller-shaped, but they have additional decorations when compared to IC87114 and PIK-39 in the form of an *ortho*-fluorophenol (SW14), a *para*-fluorophenol (SW13) or a butynol group (SW30) attached to the central pyrazolopyrimidinineamine scaffold (**Fig. 2c–e**). These groups explore the affinity pocket where they engage in hydrogen bonds with Asp787 (SW13, SW14 and SW30) and Lys779 (SW13 and SW14). Additionally, the butynol OH group of SW30 also serves as a hydrogen bond donor to the DFG Asp911 at the start of the activation loop, and the phenolic OH group of SW13 engages in hydrogen bonding with Tyr813. This set of new inhibitor-enzyme interactions leads to a substantial increase in the inhibitors' potencies toward p110δ, which is reflected in their greatly lowered half-maximal inhibitory concentration (IC_{50}) values (**Supplementary Tables 2** and **3**). The propeller shape of a compound alone does not guarantee p110δ specificity, as shown by INK666 (**Supplementary Fig. 5b**).

Our structures of p110δ in complex with SW13, SW14 and SW30 also indicate a conformational flexibility for the catalytical DFG Asp911. This residue assumes two alternative conformations in the p110δ-SW structures. One of these, the 'in' conformation, coincides with its putative ATP/Mg^{2+}-binding position (based on the p110γ-ATP complex). The other conformation has the DFG Asp911 swung away ('out' conformation). In the p110δ-SW14 and p110δ-SW30 structures, DFG Asp911 is found in the 'out' conformation, whereas in the p110δ-SW13 complex it is 'in'. In protein kinases, a shift of the DFG aspartate from the 'in' conformation (ATP-bound) to the 'out' conformation is characteristic of the catalytic cycle. By analogy, it may be that these inhibitors are inducing conformations characteristic of the PI(3)K catalytic cycle.

p110δ complexes with flat and multiselective inhibitors

ZSTK474 (ref. 44) (**8**), DL06 (**9**), DL07 (**10**), AS5 (**11**) and GDC-0941 (ref. 32) (**12**) are fairly flat compounds that do not open the specificity pocket and achieve relatively little isotype selectivity. Their binding provokes some motions of the P-loop side chains of p110δ, and these conformational changes are coordinated with changes in the conformation of the DFG Asp911 in the C-lobe.

A minimalistic approach to achieve PI(3)K inhibition

The DL06/07 series of PI(3)K inhibitors can best be described as pan-selective p110 inhibitors that represent a minimalistic approach to achieve PI(3)K inhibition (see **Supplementary Methods** for synthesis details). They are flat and small compounds with a minimal design that is just sufficient to span the adenine pocket via their pyrazolopyrimidine moiety and project into the affinity pocket by means of a phenol (DL07) or a pyridine (DL06) group attached to a propyne "stick" (**Fig. 3a**,**b**). The DL07 phenol group interacts with the DFG Asp911, forcing it to its 'in' conformation. It also induces rotations in the side chain of P-loop Met752, but not to its 'out' conformation. Similar interactions are formed by DL06.

p110δ-ZSTK474

The new pan-selective triazine PI(3)K inhibitor ZSTK474 strongly inhibits the growth of tumor cells in human cancer xenografts and therefore is a potential candidate for further clinical development[44]. Its crystal structure in complex with p110δ shows it flipped over relative to what was predicted in a computational p110γ-ZSTK474 model[44] (**Fig. 3c**). The oxygen of one of the morpholino groups is positioned as the hinge hydrogen bond acceptor, and the morpholino ring adopts a chair conformation. The benzimidazole group extends into the affinity pocket where its nitrogen acts as a hydrogen bond acceptor for the primary amine of Lys779. The difluoromethyl group points toward Pro758 in the upper wall of the hydrophobic affinity pocket. The second morpholino group adopts a somewhat twisted chair conformation and projects out of the ATP-binding pocket in the same manner as the phenyl group of LY294002 where it occupies the hydrophobic region II.

The potential of phosphate mimetics as kinase inhibitors

AS5 is a relatively flat p110α/p110δ dual-selectivity inhibitor with only modest affinities for these two isoforms. Its dimethoxyaniline group occupies the adenine pocket, where it interacts with the hinge Val828, but does not project deeply into the affinity pocket (**Fig. 3d**). It is conceivable that modifications on this scaffold that target polar moieties within the affinity pocket could increase the potencies of AS5 derivatives. Coupled to the quinoxaline group is a *p*-fluorobenzenesulfonamide, and when superimposed on the p110γ-ATP crystal structure it becomes apparent that the sulfonyl group of AS5 roughly co-localizes with the α-phosphate group of ATP. This compound reveals two strategies to mimic the ATP phosphates to achieve inhibition of p110α and p110δ. First, one of the sulfonyl oxygens of AS5 is a hydrogen bond acceptor for P-loop Ser754. Second, the fluorophenyl group exits the active site close to the DFG Asp911, in proximity of the space occupied by the β- and γ-phosphates in the p110γ-ATP structure.

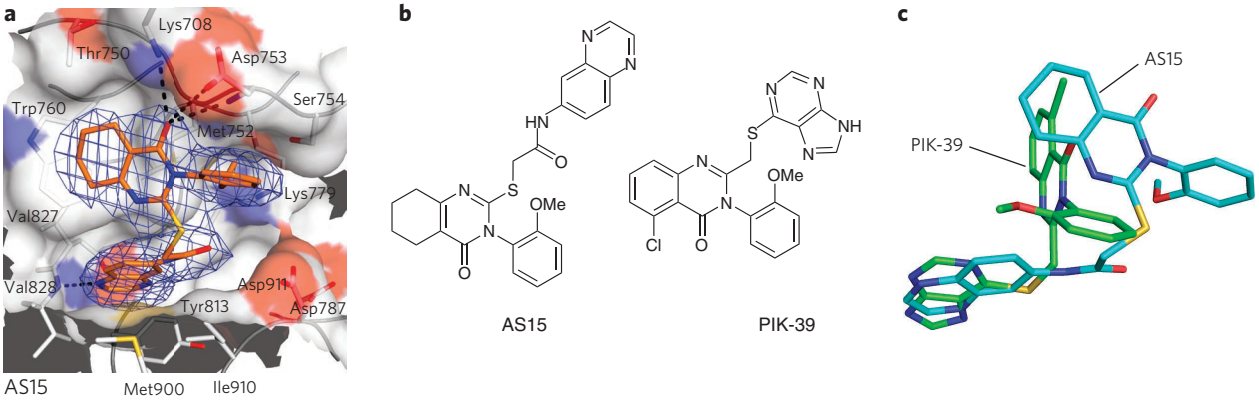

Figure 4 | Binding mode of the p110δ-selective PI(3)K inhibitor AS15 and comparison of AS15 with the propeller-shaped inhibitor PIK-39. (**a**) The highly p110δ-selective compound AS15 does not open the specificity pocket and makes extensive use of a hydrophobic patch between Trp760, Thr750 and Met752 adjacent to the adenine-binding pocket. The $2mF_o - DF_c$ contouring level is 1σ. (**b**) Chemical structures of AS15 and PIK-39. (**c**) Superposition of AS15 and PIK-39 to demonstrate their different modes of binding within the active site of p110δ.

GDC-0941 uses the space above hydrophobic region II

The identification, characterization and development of the tricyclic pyridofuropyrimidine lead PI-103 (refs. 45–47), a very potent dual-selective PI(3)K/mTOR inhibitor, has led to the pan-selective class I PI(3)K thienopyrimidine inhibitor GDC-0941, which has no off-target activity against mTOR (ref. 32). GDC-0941 is orally bioavailable and currently in phase 1 trials for the treatment of solid tumors[33].

Its structure in complex with p110δ (**Fig. 3e**) confirms the previously described binding mode to p110γ (ref. 32) but also reveals new features. Whereas the piperazine ring adopts a twisted chair conformation in the p110γ structure, it is present in a distorted boat conformation in the structure of p110δ. The terminal methanesulfonylpiperazine group is also oriented differently in both structures. In p110δ, this group is marginally tilted with respect to the central thienopyrimidine scaffold and thereby comes closer to the P-loop. Instead of the Lys802-p110γ (Arg770-p110α), the Thr750 at the equivalent position in p110δ is unable to establish a hydrogen bond to the inhibitor's sulfonyl oxygen. However, a different lysine residue (Lys708) interacts with the sulfonyl group of GDC-0941, which indicates why this compound does not lose affinity for p110δ.

AS15 explores the nonconserved rim of the active site

Although AS15 (**13**) is chemically related to the quinazolinone purine inhibitor PIK-39, its cocrystal structure with p110δ reveals an unexpected mode of binding (**Fig. 4**). Instead of wedging in between Met752 and Trp760, the hexahydroquinazolinone group presses tightly against Met752 (in its 'in' position) and Trp760. By comparing the binding modes of PIK-39 and AS15 to p110δ, three reasons can be deduced for why PIK-39, but not AS15, is able to induce the specificity pocket. First, whereas the purine group of PIK-39 acts as a hydrogen bond donor and acceptor, the AS15 quinoxaline group interacts only with the backbone amide of hinge Val828. Second, the nonplanar nature of the hexahydroquinazolinone may exceed the capacity of the specificity pocket. In its alternate location, the hexahydroquinazolinone packs into a shallow dimple formed between Met752, the small side chain of Thr750, and Trp760. In other p110 isotypes, the residue equivalent to Thr750 is a lysine or arginine. This interaction may account for the high isotype selectivity of this compound. Third, compared with the shorter thiomethyl linker of PIK-39, the longer methylthioacetamide linker of AS15 might be more conformationally restrained due to the planar nature of the linker's peptide bond. This planarity might prevent the hexahydroquinazolinone from being positioned in a way that would allow for the induction of the specificity pocket.

A number of additional p110δ-specific interactions are formed in a manner whereby the ketone oxygen from the hexahydroquinazolinone group acts as a hydrogen bond acceptor for the backbone amide of the P-loop Asp753 and for the primary amine of Lys708. The P-loop Asp753 is specific to p110δ (the corresponding residue is Ser773 in p110α and Ala805 in p110γ), and Lys708, which is located outside of the active site, has an equivalent in p110α (Lys729) but not in p110γ (Ser 760). Given that AS15 does not occupy the affinity pocket, modifications of the compound exploring this pocket should result in an increased potency for p110δ.

DISCUSSION

The p110δ-inhibitor crystal structures presented here show that selectivity can be achieved by exploiting both differences in flexibilities among the isoforms and isotype-specific contacts beyond the first shell of residues that interact with ATP. Flexibility-based inhibitors are generally able to use the inherently greater pliability of the p110δ P-loop. All propeller-shaped inhibitors create a new specificity pocket not present in the apo form of the enzyme. Small modifications of this framework (as found in AS15) can result in inhibitors that are highly selective by establishing unique p110δ-specific interactions without the formation of the specificity pocket. The plasticity of p110δ may enable this isoform to more readily accommodate even very rigid compounds. Our structures also suggest that introducing moieties interacting with the hydrophobic region II at the mouth of the active site might help to improve pharmacokinetic properties of drug-like PI(3)K inhibitors such as GDC-0941.

Initial molecular dynamic simulations suggest that allosteric pockets such as the specificity pocket can be identified with computational approaches. A similar method that imposes stress on the ATP-binding pocket may identify new strain-prone regions that could be exploited by inhibitors.

The strategy of exploring the affinity pocket is a very powerful approach to augment the potency of inhibitors while maintaining selectivity. Further development of selective inhibitors for other isotypes and for overcoming potential resistance mutations that frequently accompany treatment with inhibitors will require a broader range of PI(3)K and PIKK structures.

METHODS

Construct design, expression and purification of ΔABDp110δ. Briefly, the TEV-insertion construct of mouse p110δ was generated using the overlapping PCR method, digested with BglII and XhoI at sites encoded by the primers and ligated into pFastBac-HTa (Invitrogen) cut with the BamHI and XhoI restriction enzymes (New England Biolabs). The correct insertion of the TEV site was confirmed by DNA sequencing (amino acid sequence: 101-LVARE-(105)-ENLYFQG-(106)-GDRVKK-111). The construct has an N-terminal extension encoded by the vector (MSYHHHHHHDYDIPTTENLYFQGAMDL) preceding the first residue of p110δ. This extension has a His_6 tag and an additional vector-encoded TEV-cleavage site. Recombinant baculovirus was generated and propagated according to standard protocols. For expression, Sf9 insect cells at a density of 1×10^6 ml^{-1} were co-infected with an optimized ratio of viruses encoding the catalytic and regulatory subunit. As a regulatory subunit, we used the iSH2 fragment of the human p85α (residues 431–600), tagged with an N-terminal, noncleavable His_6 tag. The culture was incubated for 48 h after infection, and cells were harvested and washed with ice-cold phosphate-buffered saline (PBS), flash-frozen in liquid N_2 and stored at −20 °C. For purification, cell pellets corresponding to typically 8 l of culture were defrosted and resuspended in 250 ml of buffer A (20 mM Tris pH 8, 100 mM NaCl, 5% (v/v) glycerol and 2 mM β-mercaptoethanol). After addition of 2 tablets of complete EDTA-free proteinase inhibitors (Boehringer), the suspension was sonicated and the lysate was spun at 42,000 r.p.m. for 45 min. The supernatant was filtered through 0.45 µm filter units (Sartorius) and loaded onto a 5 ml HisTrap column (GE Healthcare). After a wash step with buffer A, the column was eluted using a gradient from 0–100% buffer B (buffer A + 200 mM imidazole). Fractions of the p110δ-iSH2 complex were pooled and loaded onto a 5-ml heparin column equilibrated with heparin A buffer (20 mM Tris pH 8, 100 mM NaCl, 2 mM β-mercaptoethanol). The column was washed and eluted with a gradient from 0–100% heparin B buffer (heparin A + 1 M NaCl). This chromatography step resulted in a separation of excess His_6-tagged iSH2 (earlier peak) from the p110δ-iSH2 complex (later peak). The p110δ-iSH2 fractions were pooled and adjusted to 5 mM β-mercaptoethanol. TEV proteinase at a w/w ratio of 1:10 was added, and the mixture was incubated overnight at 4 °C. After verifying that the cleavage reaction was complete, the solution was adjusted to 30 mM imidazole and passed over a second 5-ml HisTrap column to remove the ABD/His_6-iSH2, and ΔABDp110δ was collected in the flow-through. Following a concentration step using Vivaspin 20 concentrators with a 50 kDa MWCO (Vivascience), the protein was subjected to gel filtration on an S200 16/60 HiLoad column (GE Healthcare) and eluted in 20 mM Tris pH 7.2, 50 mM $(NH_4)_2SO_4$, 1% (v/v) ethylene glycol, 1% (w/v) betaine, 0.02% (w/v) CHAPS and 5 mM DTT. Finally, fractions were pooled and concentrated to 4.5–5 mg ml^{-1} as determined spectrophotometrically using the extinction coefficient 129,810 M^{-1} cm^{-1} at 280 nm, flash frozen in liquid N_2 and stored at −80 °C. We have applied this strategy to all other class IA isoforms (not shown).

Synthesis and characterization of SW13, SW14, SW30, DL06 and DL07. A detailed description of the synthesis and characterization of these compounds can be found in the **Supplementary Methods**.

X-ray crystallography. High-quality diffraction data of ΔABDp100δ crystals grown in the presence of inhibitors were obtained using a microseeding protocol implemented on our robotic setup. All crystal structures were solved by molecular replacement. See **Supplementary Methods** for additional details.

Lipid kinase activity assay. To compare the PI(3)K lipid kinase activity of the crystallized mouse ΔABDp110δ construct with that of the full-length mouse p110δ–mouse p85α complex and the mouse p110δ–human p85α nicSH2 construct, a Transcreener ADP assay (Bellbrook Labs) was performed according to the manufacturer's instructions. Briefly, for the generation of the ADP/ATP

standard curve, 10 µl of a 60 µM ADP/ATP (2×) mixture of various ADP:ATP concentrations were mixed with 5 µl of anti-ADP antibody at 80 µg ml^{-1} (4×) and 5 µl of ADP Alexa633 tracer at 40 nM (4×) in a low-volume, black and round bottom 384-well plate (Corning). The plate was protected from light and shaken at 500 r.p.m. for 1 h before polarization measurements using a PHERAstar (BMG Labtech) fluorescence polarization microplate reader (λ_{exc} = 612 nm, λ_{em} = 670 nm). For the kinase reaction, 10 nM of enzymes were incubated for 1 h at 25 °C in a buffer consisting of 50 mM HEPES (pH 7.5), 4 mM $MgCl_2$, 2 mM EGTA and 30 µM diC_8-PIP_2 (Echelon). The reaction was started by the addition of 30 µM ATP (Sigma-Aldrich, neutralized). The control included the same components with the exception of the diC_8PIP_2 substrate. The reaction was stopped by mixing 10 µl of the kinase reaction with 10 µl of the Stop & Detect buffer (20 mM HEPES pH 7.5, 40 mM EDTA, 0.2% (w/v) Brij-35) containing 20 nM ADP Alexa633 tracer (2×) and 40 µg ml^{-1} ADP antibody (2×). To allow for signal stabilization, the plate was shaken at 500 r.p.m. for 1 h before fluorescence polarization measurements. The data were plotted and fitted in Kaleidagraph (Synergy Software) using an exponential decay function.

Accession codes. Protein Data Bank: Coordinates of all p110δ structures and accompanying structure factors have been deposited under the following accession codes: 2X38 (p110δ-IC87114), 2WXF (p110δ–PIK-39), 2WXG (p110δ-SW13), 2WXH (p110δ-SW14), 2WXI (p110δ-SW30), 2WXJ (p110δ-INK654), 2WXK (p110δ-INK666), 2WXL (p110δ-ZSTK474), 2WXM (p110δ-DL06), 2WXN (p110δ-DL07), 2WXO (p110δ-AS5), 2WXP (p110δ–GDC-0941), 2WXQ (p110δ-AS15) and 2WXR (apo-p110δ). The structure of the p110γ-ATP complex (entry 1E8X) was deposited as part of a previous study.

Received 18 September 2009; accepted 30 November 2009; published online 10 January 2010; corrected after print 12 February 2010 and 2 March 2010

References

1. Vanhaesebroeck, B. *et al.* Synthesis and function of 3-phosphorylated inositol lipids. *Annu. Rev. Biochem.* **70**, 535–602 (2001).
2. Zhao, L. & Vogt, P.K. Class I PI3K in oncogenic cellular transformation. *Oncogene* **27**, 5486–5496 (2008).
3. Manning, B.D. & Cantley, L.C. AKT/PKB signaling: navigating downstream. *Cell* **129**, 1261–1274 (2007).
4. Sundstrom, T.J., Anderson, A.C. & Wright, D.L. Inhibitors of phosphoinositide-3-kinase: a structure-based approach to understanding potency and selectivity. *Org. Biomol. Chem.* **7**, 840–850 (2009).
5. Miled, N. *et al.* Mechanism of two classes of cancer mutations in the phosphoinositide 3-kinase catalytic subunit. *Science* **317**, 239–242 (2007).
6. Domin, J. & Waterfield, M.D. Using structure to define the function of phosphoinositide 3-kinase family members. *FEBS Lett.* **410**, 91–95 (1997).
7. Vanhaesebroeck, B. & Waterfield, M.D. Signaling by distinct classes of phosphoinositide 3-kinases. *Exp. Cell Res.* **253**, 239–254 (1999).
8. Walker, E.H., Perisic, O., Ried, C., Stephens, L. & Williams, R.L. Structural insights into phosphoinositide 3-kinase catalysis and signalling. *Nature* **402**, 313–320 (1999).
9. Katso, R. *et al.* Cellular function of phosphoinositide 3-kinases: implications for development, homeostasis, and cancer. *Annu. Rev. Cell Dev. Biol.* **17**, 615–675 (2001).
10. Cantley, L.C. The phosphoinositide 3-kinase pathway. *Science* **296**, 1655–1657 (2002).
11. Chantry, D. *et al.* p110delta, a novel phosphatidylinositol 3-kinase catalytic subunit that associates with p85 and is expressed predominantly in leukocytes. *J. Biol. Chem.* **272**, 19236–19241 (1997).
12. Vanhaesebroeck, B. *et al.* P110delta, a novel phosphoinositide 3-kinase in leukocytes. *Proc. Natl. Acad. Sci. USA* **94**, 4330–4335 (1997).
13. Ghigo, A. & Hirsch, E. Isoform selective phosphoinositide 3-kinase gamma and delta inhibitors and their therapeutic potential. *Recent Pat. Inflamm. Allergy Drug Discov.* **2**, 1–10 (2008).
14. Samuels, Y. *et al.* High frequency of mutations of the PIK3CA gene in human cancers. *Science* **304**, 554 (2004).
15. Kang, S., Denley, A., Vanhaesebroeck, B. & Vogt, P.K. Oncogenic transformation induced by the p110beta, -gamma, and -delta isoforms of class I phosphoinositide 3-kinase. *Proc. Natl. Acad. Sci. USA* **103**, 1289–1294 (2006).
16. Hickey, F.B. & Cotter, T.G. BCR-ABL regulates phosphatidylinositol 3-kinase-p110gamma transcription and activation and is required for proliferation and drug resistance. *J. Biol. Chem.* **281**, 2441–2450 (2006).
17. Sujobert, P. *et al.* Essential role for the p110delta isoform in phosphoinositide 3-kinase activation and cell proliferation in acute myeloid leukemia. *Blood* **106**, 1063–1066 (2005).
18. Knight, Z.A. *et al.* A pharmacological map of the PI3-K family defines a role for p110alpha in insulin signaling. *Cell* **125**, 733–747 (2006).
19. Jackson, S.P. *et al.* PI 3-kinase p110beta: a new target for antithrombotic therapy. *Nat. Med.* **11**, 507–514 (2005).
20. Rommel, C., Camps, M. & Ji, H. PI3K delta and PI3K gamma: partners in crime in inflammation in rheumatoid arthritis and beyond? *Nat. Rev. Immunol.* **7**, 191–201 (2007).
21. Takeda, M. *et al.* Allergic airway hyperresponsiveness, inflammation, and remodeling do not develop in phosphoinositide 3-kinase gamma-deficient mice. *J. Allergy Clin. Immunol.* **123**, 805–812 (2009).
22. Park, S.J., Min, K.H. & Lee, Y.C. Phosphoinositide 3-kinase delta inhibitor as a novel therapeutic agent in asthma. *Respirology* **13**, 764–771 (2008).
23. Knight, Z.A. & Shokat, K.M. Chemically targeting the PI3K family. *Biochem. Soc. Trans.* **35**, 245–249 (2007).
24. Ameriks, M.K. & Venable, J.D. Small molecule inhibitors of phosphoinositide 3-kinase (PI3K) delta and gamma. *Curr. Top. Med. Chem.* **9**, 738–753 (2009).
25. Vlahos, C.J., Matter, W.F., Hui, K.Y. & Brown, R.F. A specific inhibitor of phosphatidylinositol 3-kinase, 2-(4- morpholinyl)-8-phenyl-4h-1-benzopyran-4-one (Ly294002). *J. Biol. Chem.* **269**, 5241–5248 (1994).
26. Arcaro, A. & Wymann, M.P. Wortmannin is a potent phosphatidylinositol 3-kinase inhibitor: the role of phosphatidylinositol 3,4,5-trisphosphate in neutrophil responses. *Biochem. J.* **296**, 297–301 (1993).
27. Yu, K. *et al.* PWT-458, a novel pegylated-17-hydroxywortmannin, inhibits phosphatidylinositol 3-kinase signaling and suppresses growth of solid tumors. *Cancer Biol. Ther.* **4**, 538–545 (2005).
28. Ihle, N.T. *et al.* Molecular pharmacology and antitumor activity of PX-866, a novel inhibitor of phosphoinositide-3-kinase signaling. *Mol. Cancer Ther.* **3**, 763–772 (2004).
29. Walker, E.H. *et al.* Structural determinants of phosphoinositide 3-kinase inhibition by wortmannin, LY294002, quercetin, myricetin, and staurosporine. *Mol. Cell* **6**, 909–919 (2000).
30. Camps, M. *et al.* Blockade of PI3Kgamma suppresses joint inflammation and damage in mouse models of rheumatoid arthritis. *Nat. Med.* **11**, 936–943 (2005).
31. Apsel, B. *et al.* Targeted polypharmacology: discovery of dual inhibitors of tyrosine and phosphoinositide kinases. *Nat. Chem. Biol.* **4**, 691–699 (2008).
32. Folkes, A.J. *et al.* The identification of 2-(1H-indazol-4-yl)-6-(4-methanesulfonyl-piperazin-1-ylmethyl)-4-morpholin-4-yl-thieno[3,2-d] pyrimidine (GDC-0941) as a potent, selective, orally bioavailable inhibitor of class I PI3 kinase for the treatment of cancer. *J. Med. Chem.* **51**, 5522–5532 (2008).
33. Raynaud, F.I. *et al.* Biological properties of potent inhibitors of class I phosphatidylinositide 3-kinases: from PI-103 through PI-540, PI-620 to the oral agent GDC-0941. *Mol. Cancer Ther.* **8**, 1725–1738 (2009).
34. Maira, S.M. *et al.* Identification and characterization of NVP-BEZ235, a new orally available dual phosphatidylinositol 3-kinase/mammalian target of rapamycin inhibitor with potent *in vivo* antitumor activity. *Mol. Cancer Ther.* **7**, 1851–1863 (2008).
35. Garlich, J.R. *et al.* A vascular targeted pan phosphoinositide 3-kinase inhibitor prodrug, SF1126, with antitumor and antiangiogenic activity. *Cancer Res.* **68**, 206–215 (2008).
36. Sadhu, C., Masinovsky, B., Dick, K., Sowell, C.G. & Staunton, D.E. Essential role of phosphoinositide 3-kinase delta in neutrophil directional movement. *J. Immunol.* **170**, 2647–2654 (2003).
37. Huang, C.H. *et al.* The structure of a human p110alpha/p85alpha complex elucidates the effects of oncogenic PI3Kalpha mutations. *Science* **318**, 1744–1748 (2007).
38. Kornev, A.P., Haste, N.M., Taylor, S.S. & Eyck, L.F. Surface comparison of active and inactive protein kinases identifies a conserved activation mechanism. *Proc. Natl. Acad. Sci. USA* **103**, 17783–17788 (2006).
39. Rodriguez-Viciana, P. *et al.* Phosphatidylinositol-3-OH kinase as a direct target of Ras. *Nature* **370**, 527–532 (1994).
40. Pacold, M.E. *et al.* Crystal structure and functional analysis of Ras binding to its effector phosphoinositide 3-kinase gamma. *Cell* **103**, 931–943 (2000).
41. Mandelker, D. *et al.* A frequent kinase domain mutation that changes the interaction between PI3Kalpha and the membrane. *Proc. Natl. Acad. Sci. USA* **106**, 16996–17001 (2009).
42. Williams, R., Berndt, A., Miller, S., Hon, W.C. & Zhang, X. Form and flexibility in phosphoinositide 3-kinases. *Biochem. Soc. Trans.* **37**, 615–626 (2009).
43. Williams, O. *et al.* Discovery of dual inhibitors of the immune cell PI3Ks p110δ and p110γ: a prototype for new anti-inflammatory drugs. *Chem. Biol.* (in the press).
44. Yaguchi, S. *et al.* Antitumor activity of ZSTK474, a new phosphatidylinositol 3-kinase inhibitor. *J. Natl. Cancer Inst.* **98**, 545–556 (2006).
45. Fan, Q.W. *et al.* A dual PI3 kinase/mTOR inhibitor reveals emergent efficacy in glioma. *Cancer Cell* **9**, 341–349 (2006).
46. Hayakawa, M. *et al.* Synthesis and biological evaluation of pyrido[3′,2′:4,5] furo[3,2-d]pyrimidine derivatives as novel PI3 kinase p110alpha inhibitors. *Bioorg. Med. Chem. Lett.* **17**, 2438–2442 (2007).
47. Raynaud, F.I. *et al.* Pharmacologic characterization of a potent inhibitor of class I phosphatidylinositide 3-kinases. *Cancer Res.* **67**, 5840–5850 (2007).

Acknowledgments

We thank the beamline scientists and members of staff at the European Synchrotron Radiation Facility beamlines ID14-1, ID14-2, ID14-4, ID23-1, ID29 and BM30A (Grenoble, France), the Swiss Light Source beamline X06SA (Villigen, Switzerland) and the Diamond beamline I02 (Oxfordshire, UK). We are grateful to M. Allen for collecting the p110δ-ZSTK474 dataset and to O. Perisic for her help with the manuscript and for numerous contributions to this study. Part of this material is based on work supported under a US National Science Foundation Graduate Research Fellowship to O.W. and was supported by the Graduate Research and Education in Adaptive bio-Technology Training Program of the University of California Systemwide Biotechnology Research and Education Program, grant number 2008-005 to O.W. A.B. is supported by Merck-Serono, Geneva.

Author contributions

A.B. expressed and purified the ΔABDp110δ construct, crystallized the first ΔABDp110δ-inhibitor complexes, collected datasets, determined and refined their structures and performed the kinase activity assay. S.M. helped in the purification, crystallization and structure determination and refinement of several ΔABDp110δ-inhibitor complexes. O.W., D.D.L. and B.T.H. synthesized and characterized the inhibitors SW13, SW14, SW30, DL06 and DL07 with input from K.M.S. and determined their IC_{50} values. J.I.P. performed the molecular dynamics and free energy perturbation experiments. F.G. devised and provided access to the Morpheus Screen and helped with the implementation of a microseeding protocol. W.-C.H. helped with the insect cell culture and crystal data collection. P.R., Y.L. and C.R. designed and characterized the inhibitors INK654 and INK666. P.G., T.R., M.K.S. and J.P.S. synthesized and characterized the inhibitors AS5 and AS15 and helped with large-scale insect cell expression. J.P.S. also provided valuable advice and support throughout the project. R.L.W. helped with the crystal data collection, the structure determination and refinement and the preparation of the movies. The manuscript was written by R.L.W. and A.B.

Competing interests statement

The authors declare competing financial interests: details accompany the full-text HTML version of the paper at http://www.nature.com/naturechemicalbiology/.

Additional information

Supplementary information and chemical compound information is available online at http://www.nature.com/naturechemicalbiology/. Reprints and permissions information is available online at http://npg.nature.com/reprintsandpermissions/. Correspondence and requests for materials should be addressed to R.L.W.

CORRIGENDUM

The p110δ structure: mechanisms for selectivity and potency of new PI(3)K inhibitors

Alex Berndt, Simon Miller, Olusegun Williams, Daniel D Le, Benjamin T Houseman, Joseph I Pacold, Fabrice Gorrec, Wai-Ching Hon, Pingda Ren, Yi Liu, Christian Rommel, Pascale Gaillard, Thomas Rückle, Matthias K Schwarz, Kevan M Shokat, Jeffrey P Shaw & Roger L Williams

Nat. Chem. Biol. **6**, 117–124 (2010); published online 10 January 2010; corrected after print 12 February 2010 and 2 March 2010

In the version of this article initially published, the structure of p110δ in complex with the inhibitor IC87114 was refined with an incorrect inhibitor structure (original Protein Data Bank accession code 2WXE). The structure has now been refined with the correct inhibitor structure and redeposited in the PDB with accession code 2X38. The structural image in Fig. 2a and the PDB accession code in the Methods section of the paper have been corrected in the HTML and PDF versions of the article.

CORRIGENDUM

Revealing the delta lady

Paul Workman & Rob L M van Montfort

Nat. Chem. Biol. **6,** 82–83 (2010); published online 15 January 2010; corrected after print 2 March 2010

In the version of this article initially published, there was an error in the chemical structure of IC87114 that arose from the coordinates used to generate Figure 1a. The corrected structure has been deposited by Berndt *et al.* to the Protein Data Bank (PDB code 2X38). Figure 1a and the PDB code in the figure legend have been corrected in the HTML and PDF versions of the article.

CORRIGENDUM

An upfront investment

Damian W Young

Nat. Chem. Biol. **6**, 174–175 (2010); published online 12 February 2010; corrected after print 18 March 2010

In the version of this article initially published, the palladium catalyst was incorrectly drawn as $PdPh_4$. The molecular formula is actually $Pd(PPh_3)_4$. The error has been corrected in the HTML and PDF versions of the article.

ERRATUM

Cover caption

Nat. Chem. Biol. **6** (2010); published online 12 February 2010; corrected after print 18 March 2010

In the version of this cover caption initially published, Sigrid Hart's name was misspelled. The error has been corrected in the HTML and PDF versions of the cover caption.

ERRATUM

Garbled messages and corrupted translations

Tilman Schneider-Poetsch, Takeo Usui, Daisuke Kaida & Minoru Yoshida

Nat. Chem. Biol. **6**, 189–198 (2010); published online 12 February 2010; corrected after print 18 March 2010

In the version of this article initially published, the page numbers in reference 69 were incorrect. The error has been corrected in the HTML and PDF versions of the article.